Role of evanescent wave in valley polarization through junction of mono- and bi-layer graphenes

Takeshi Nakanishi[1], Mikito Koshino[2,3] and Tsuneya Ando[2]

[1]Nanosystem Research Institute, AIST, 1–1–1 Umezono, Tsukuba 305-8568, Japan
[2]Department of Physics, Tokyo Institute of Technology, 2–12–1 Ookayama, Meguro-ku, Tokyo 152-8551, Japan

E-mail: `t.nakanishi@aist.go.jp`

Abstract. The origin of strong valley polarization of electron wave transmitted through boundary between mono- and bi-layer graphenes can be ascribed to an evanescent wave in the bilayer graphene. The valley polarization is further enhanced across a ribbon-like region formed by partially overlapping of two monolayer graphenes.

Graphene consists of a two-dimensional hexagonal crystal of carbon atoms, in which electron dynamics is governed by the Dirac equation [1]. The electronic states have various intriguing features. In fact, the wave functions are characterized by spinor whose orientation is inextricably linked to the direction of the electron momentum in a different manner between monolayer and bilayer graphenes [2, 3, 4]. The purpose of this paper is to elucidate the origin of valley polarization [8] induced in transmission probability through the boundary between monolayer and bilayer graphenes.

In graphenes, states associated with K and K' points or valleys are degenerate. In a graphene sheet with a finite width, localized edge states are formed, when the boundary is in a certain specific direction under appropriate conditions, and only a single right- and left-going wave can carry current at each of the K and K' points [5]. A way to make valley filtering has been proposed with the explicit use of this fact [6]. Edge states in bilayer graphene were also studied [7].

We consider a straight boundary (with zigzag form) of monolayer and bilayer graphenes arranged in the AB (Bernal) stacking as illustrated in Fig. 1 and we choose the y axis along the boundary. Electronic states are described in an effective-mass scheme. In monolayer graphene, a unit cell contains two carbon atoms denoted by A and B, and for states in the vicinity of the K point, the Schrödinger equation and the corresponding wave function are given by

$$\gamma(\vec{\sigma}\cdot\hat{\mathbf{k}})\mathbf{F}^K(\mathbf{r}) = \varepsilon\mathbf{F}^K(\mathbf{r}), \quad \mathbf{F}^K(\mathbf{r}) = \begin{pmatrix} F_A^K(\mathbf{r}) \\ F_B^K(\mathbf{r}) \end{pmatrix} = \begin{pmatrix} se^{-i\theta} \\ 1 \end{pmatrix} e^{i\mathbf{k}\cdot\mathbf{r}}, \tag{1}$$

where γ is a band parameter, $\hat{\mathbf{k}} = (\hat{k}_x, \hat{k}_y) = -i\vec{\nabla}$ a wave vector operator, $(k_x, k_y) = k(\cos\theta, \sin\theta)$ a wave vector, $s = +1$ and -1 for the conduction and valence band, respectively, σ_x and σ_y the Pauli matrices, and F_A^K and F_B^K slowly-varying envelope functions describing amplitudes at A and B sites, respectively [1].

[3] Present address: Department of Physics, Tohoku University, Sendai 980-8578, Japan

In a bilayer graphene, the bottom layer is denoted as 1 and the top layer as 2. A unit cell contains two carbon atoms denoted by A_1 and B_1 in layer 1, and A_2 and B_2 in layer 2. For the inter-layer coupling, we include coupling γ_1 between vertically neighboring atoms B_1 and A_2. The Schrödinger equation becomes

$$\begin{pmatrix} \gamma(\vec{\sigma}\cdot\hat{\mathbf{k}}) & \frac{1}{2}\gamma_1\sigma_- \\ \frac{1}{2}\gamma_1\sigma_+ & \gamma(\vec{\sigma}\cdot\hat{\mathbf{k}}) \end{pmatrix} \mathbf{F}^K(\mathbf{r}) = \varepsilon \mathbf{F}^K(\mathbf{r}), \tag{2}$$

where $\sigma_\pm = \sigma_x \pm i\sigma_y$ and $\mathbf{F}^K(\mathbf{r})$ is a four component vector consisting of F^K_{A1}, F^K_{B1}, F^K_{A2}, and F^K_{B2}.

In the energy region close to the Dirac point $\gamma k/\gamma_1 \to 0$, wave functions are mainly described by two major components on A1 and B2, and other minor components are small due to the interlayer couplings and can be eliminated. In addition to a traveling mode denoted by $\tilde{\mathbf{F}}^K$, we have evanescent modes $\mathbf{G}^K$ decaying or growing exponentially in the positive x direction in low energy region $|\varepsilon| < \gamma_1$. The major components of the traveling mode and the decaying evanescent mode are given by

$$\begin{pmatrix} \tilde{F}^K_{A1} \\ \tilde{F}^K_{B2} \end{pmatrix} = \begin{pmatrix} se^{-2i\theta} \\ 1 \end{pmatrix} e^{i\mathbf{k}\cdot\mathbf{r}}, \quad \begin{pmatrix} G^K_{A1} \\ G^K_{B2} \end{pmatrix} = \begin{pmatrix} s\gamma(\kappa_x - k_y)/\gamma_1 \\ \gamma(\kappa_x + k_y)/\gamma_1 \end{pmatrix} e^{-\kappa_x x + ik_y y}, \tag{3}$$

with $\kappa_x = \sqrt{|\varepsilon|(\gamma_1 - |\varepsilon|)/\gamma^2 + k_y^2}$. For the traveling mode, the wave function for $k_y < 0$ is complex conjugate of that for $k_y > 0$. For the evanescent mode, however, the absolute value of the amplitude is quite asymmetric between positive and negative k_y. This asymmetry can be seen by ratio G^K_{A1}/G^K_{B2} shown in the upper panel in Fig. 2.

For the K' point the Schrödinger equations are obtained by replacing $\hat{k}_y$ with $-\hat{k}_y$ and therefore the wave functions by replacing k_y with $-k_y$ in both monolayer and bilayer graphenes. Therefore, the asymmetry of $G^{K'}_{A1}/G^{K'}_{B2}$ for the K' point is opposite to that of the K point. This asymmetry is the origin of valley polarization of transmitted wave, as will be shown below.

We can derive the boundary condition for wave functions $\mathbf{F}^K$ and $\mathbf{F}^{K'}$, using their relation to the amplitude of the wave function in a tight-binding model [1]. The results for the boundary shown in Fig. 1 (a) are [8]

$$\text{(i) } F^\upsilon_{A1}(0,y) = F^\upsilon_A(0,y); \quad \text{(ii) } F^\upsilon_{B1}(0,y) = F^\upsilon_B(0,y); \quad \text{(iii) } F^\upsilon_{B2}(0,y) = 0, \tag{4}$$

where $\upsilon = K, K'$. These conditions do not cause mixing between the K and K' points, leading to the absence of inter-valley transmission through the boundary.

We consider transmission of electron wave injected from the K valley in the monolayer side at the Fermi level in an oblique direction with wave vector $\mathbf{k}$ in the case that electron concentration is the same in the monolayer and bilayer graphenes. The transmission of the electron wave through the boundary can explicitly be calculated by considering right- and left-going traveling modes in the monolayer graphene and a right-going traveling mode and an evanescent mode decaying in the positive x direction in the bilayer graphene.

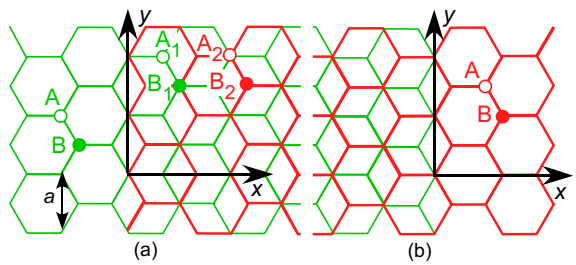

Figure 1. Atomic structure near boundaries between monolayer and bilayer graphene. Red (thick) and green (thin) lines represent the top layer with A_2 and B_2 sites, and bottom layer with A_1 and B_1 sites, respectively.

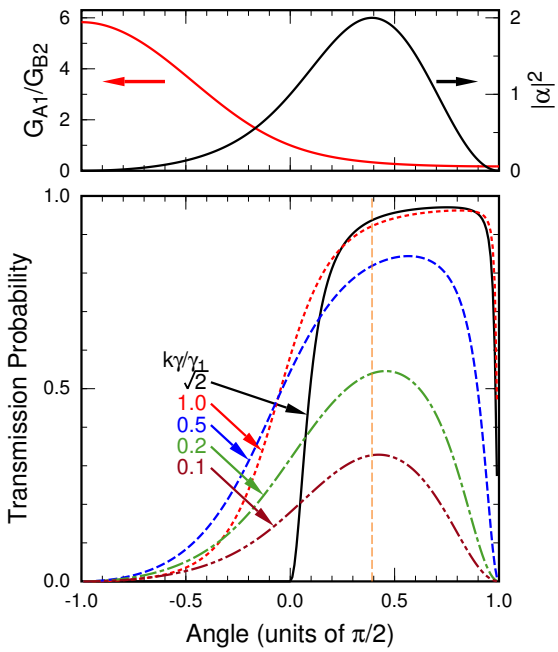

Figure 2. Upper panel: Ratio of G^K_{A1}/G^K_{B2} of the evanescent wave and $|\alpha|^2$ in the limit $k \to 0$. Lower panel: Calculated transmission probability for several charge densities specified by k in the monolayer graphene. The vertical dotted line shows θ_0 in the limit $k \to 0$.

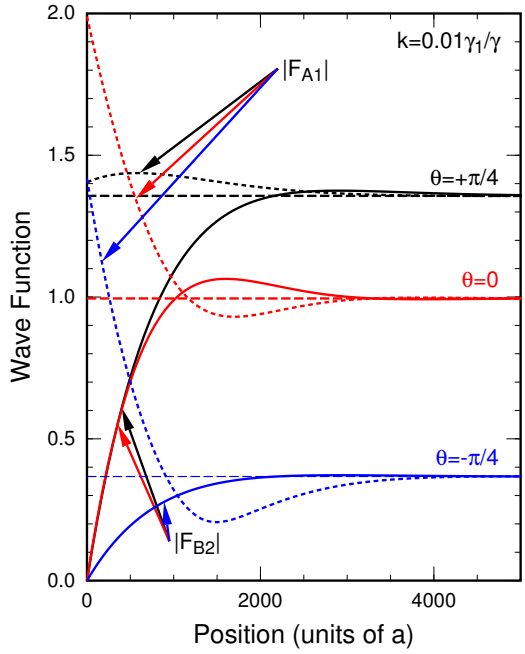

Figure 3. Calculated wave function in bilayer graphene near a boundary for incident angle $\theta = -\pi/4$, 0, and $+\pi/4$. The amplitude is normalized by that of the incident wave.

In the low energy region $\gamma k/\gamma_1 \to 0$, an approximate boundary condition is straightforwardly written down for wave functions in monolayer graphene and major components in bilayer graphene [8]. First, we note that $F^v_B(0,y)$ vanishes, because of the condition (ii) of (4) and F^v_{B1} becomes negligible for $\varepsilon \to 0$. With the use of wavefunctions (1) for incident and reflected waves, we immediately see that the reflection coefficient becomes $r_K = -1$ and therefore $F^v_A(0,y) = 2e^{ik_y y}\cos\theta$ for $k \to 0$. Then, the remaining conditions (i) and (iii) are written as

$$\alpha \tilde{F}^v_{A1}(0,y) + \beta G^v_{A1}(0,y) = F^v_A(0,y), \quad \alpha \tilde{F}^v_{B2}(0,y) + \beta G^v_{B2}(0,y) = 0. \tag{5}$$

Then, we immediately have

$$|\alpha|^2 = \frac{4\cos^2\theta}{1 + 2(G_{A1}/G_{B2})\cos(2\theta) + (G_{A1}/G_{B2})^2}, \tag{6}$$

which is also shown in the upper panel in Fig. 2. The amplitude is suppressed for $\theta < 0$ and enhanced for $\theta > 0$, corresponding to the asymmetry of G^K_{A1}/G^K_{B2}. Apart from this asymmetry, the wave function has considerable amplitude in the bilayer except at $\theta = \pm\pi/2$ in spite of the fact $r_K = -1$.

The transmission probability $T^K(\theta)$ is obtained by multiplying $|\alpha|^2$ by the ratio of the group velocity. Then, $T^K(\theta)$ vanishes for $k \to 0$ and increases in proportion to k, because the velocity is proportional to k in the bilayer side but constant in monolayer side. It takes a maximum at $\theta = s\theta_0$, with $\theta_0 = \sin^{-1}(1/\sqrt{3}) \approx 0.196\pi$. For the K' point, $T_{K'}$ is obtained by replacing θ with $-\theta$. The opposite asymmetry between the K and K' points gives rise to strong valley polarization across the interface of monolayer and bilayer graphenes.

The lower panel in Fig. 2 shows an example of calculated transmission probability as a function of incident angle θ. The electron density is specified by k corresponding to the Fermi energy in the monolayer and the results in the low-density regime $\gamma k/\gamma_1 \leq \sqrt{2}$ are shown. At the bottom of the first excited conduction band, i.e., $k\gamma/\gamma_1 = \sqrt{2}$, the transmission completely vanishes in the region $\theta \leq 0$. This is closely related to the presence of a perfectly reflecting state, which emerges only for the zigzag boundary [8]. For sufficiently small $k\gamma/\gamma_1$, the result agrees with approximate $T^K(\theta)$ obtained above.

Figure 3 shows some examples of the wave function on A1 (dotted lines) and B2 (solid lines) sites in the bilayer graphene as a function of position along incident direction θ. At the boundary chosen as the origin, F_{B2} vanishes and $|F_{A1}| = \sqrt{2}$ and 0 for $\theta = \pm\pi/4$ and 0, respectively, in the low energy region $\gamma k/\gamma_1 \ll 1$. The wave functions consist of traveling and evanescent waves, and the boundary conditions are satisfied by the presence of considerable amplitude of the evanescent mode. In fact, the spatially-varying amplitude in the bilayer graphene mostly consists of the evanescent mode. The constant amplitude at the position away from the boundary corresponds to amplitude $|\alpha|$ of the transmitted wave. It is small for $\theta = -\pi/4$ than that for $\theta = +\pi/4$ as discussed above.

Next, we consider an interface shown in Fig. 1 (b), i.e., opposite to that shown in Fig. 1 (a). The boundary conditions become

$$F^{\upsilon}_{A2}(0,y) = F^{\upsilon}_{A}(0,y); \quad F^{\upsilon}_{B2}(0,y) = F^{\upsilon}_{B}(0,y); \quad F^{\upsilon}_{A1}(0,y) = 0, \tag{7}$$

giving $T_K(\theta)$ same as that for interface (a) for the transmission probability from the bilayer into the monolayer with incident angle θ. The situation is the same for boundaries with other three kinds of atomic structure of zigzag or armchair considered previously [8]. This may be derived with the use of symmetry relation between (a) and (b), although not discussed here.

The valley polarization of waves transmitted through a single boundary is increased when waves go through a ribbon-shaped bilayer region formed by partially overlapping monolayer graphenes, i.e., when (a) and (b) in Fig. 1 are connected with each other, In fact, the total transmission probability through the bilayer ribbon becomes $\propto T^K(\theta)^2$, when interference effects are neglected [9]. This is quite in contrast to the case that a ribbon-shaped monolayer graphene is placed on top of a monolayer graphene, where the valley polarization nearly cancels out after transmission through two boundaries [8].

In conclusion, the significant valley polarization of transmitted waves through a boundary between monolayer and bilayer graphenes is ascribed to the evanescent wave in the bilayer graphene possessing strong asymmetry between the K and K' points. Further, the valley polarization can be accumulated in sequence of appropriate types of boundaries.

This work was supported in part by Grant-in-Aid for Scientific Research on Priority Area "Carbon Nanotube Nanoelectronics," by Grant-in-Aid for Scientific Research, and by GCOE Program at Tokyo Tech "Nanoscience and Quantum Physics" from Ministry of Education, Culture, Sports, Science and Technology Japan.

References

[1] T. Ando, J. Phys. Soc. Jpn. **74**, 777 (2005).
[2] T. Ando, T. Nakanishi, and R. Saito, J. Phys. Soc. Jpn. **67**, 2857 (1998).
[3] E. McCann and V. I. Falko, Phys. Rev. Lett. **96**, 086805 (2006).
[4] M. Koshino and T. Ando, Phys. Rev. B **73**, 245403 (2006).
[5] M. Fujita, K. Wakabayashi, K. Nakada. and K. Kusakabe, J. Phys. Soc. Jpn. **65**, 1920 (1996).
[6] A. Rycerz, J. Tworzydo, and C. W. J. Beenakker, Nat. Phys. **3**, 172 (2007).
[7] E. V. Castro, N. M. R. Peres, J. M. B. Lopes dos Santos, A. H. Castro Neto, and F. Guinea, Phys. Rev. Lett. **100**, 026802 (2008).
[8] T. Nakanishi, M. Koshino, and T. Ando, Phys. Rev. B **82**, 125428 (2010).
[9] J. W. Gonzalez, H. Santos, M. Pacheco, L. Chico, and L. Brey, Phys. Rev. B **81**, 195406 (2010).